Yields of Clustered DNA Damage Induced by Charged-Particle Radiations of Similar Kinetic Energy per Nucleon: LET Dependence in Different DNA Microenvironments

Authors: Keszenman, Deborah J., and Sutherland, Betsy M.

Yields of Clustered DNA Damage Induced by Charged-Particle Radiations of Similar Kinetic Energy per Nucleon: LET Dependence in Different DNA Microenvironments[1]

Deborah J. Keszenman[2] and Betsy M. Sutherland

Biology Department, Brookhaven National Laboratory, Upton, New York 11973

Keszenman, D. J. and Sutherland, B. M. Yields of Clustered DNA Damage Induced by Charged-Particle Radiations of Similar Kinetic Energy per Nucleon: LET Dependence in Different DNA Microenvironments. *Radiat. Res.* 174, 238–250 (2010).

To determine the linear energy transfer (LET) dependence of the biological effects of densely ionizing radiation in relation to changes in the ionization density along the track, we measured the yields and spectrum of clustered DNA damages induced by charged particles of different atomic number but similar kinetic energy per nucleon in different DNA microenvironments. Yeast DNA embedded in agarose in solutions of different free radical scavenging capacity was irradiated with 1 GeV protons, 1 GeV/ nucleon oxygen ions, 980 MeV/nucleon titanium ions or 968 MeV/nucleon iron ions. The frequencies of double-strand breaks (DSBs), abasic sites and oxypurine clusters were quantified. The total DNA damage yields per absorbed dose induced in non-radioquenching solution decreased with LET, with minor variations in radioquenching conditions being detected. However, the total damage yields per particle fluence increased with LET in both conditions, indicating a higher efficiency per particle to induce clustered DNA damages. The yields of DSBs and non-DSB clusters as well as the damage spectra varied with LET and DNA milieu, suggesting the involvement of more than one mechanism in the formation of the different types of clustered damages. © 2010 by Radiation Research Society

INTRODUCTION

Humans may be exposed to densely ionizing radiations in extraterrestrial as well as terrestrial environments. In space, one of the fundamental hazards for humans is the exposure to charged particles such as protons and heavy ions (HZE) of different atomic number (*Z*) and energies. On Earth, charged-particle beams consisting of protons or carbon ions are increasingly being used for tumor therapy (*1*). As a result of exposure to ionizing radiation, a variety of DNA alterations are induced, including bistranded clustered lesions (*2*).

Clustered DNA damage is defined as two or more strand breaks, oxidized bases or abasic sites within a few helical turns. These types of lesions are produced in both isolated and cellular DNA (*2–4*). In human cells, it has been shown that they are induced at doses as low as 10 cGy from high- or low-linear energy transfer (LET) radiations (*2, 5*). Clustered DNA lesions are also produced spontaneously during normal cell oxidative metabolism as well as a consequence of exposure to bleomycin, an oxidizing radiomimetic drug widely used in cancer therapy (*6–8*).

Several lines of evidence indicate that clustered DNA damages are difficult to repair and that the efficiency of the repair processes depends on the level, structure and complexity of the damage. Using fluorophore-labeled oligonucleotides containing abasic clusters, Paap *et al.* (*9*) showed that spatial arrangement within the cluster determines the efficiency of repair by Ape1 enzyme and that bipolar clusters (one strand lesion 3′ and one lesion 5′ opposing from the reference abasic site) are highly refractory to repair. In addition, Asaithamby *et al.* (*10*) observed that γ-H2AX foci in iron-ion-irradiated cells persisted for 48 h postirradiation, indicating the existence of unrepaired DSBs. In several biological systems, including prokaryotic and mammalian cells and synthetic oligonucleotides containing clustered DNA alterations, it has been demonstrated that *de novo* double-strand breaks (DSBs) can be generated during the repair of some DNA clustered lesions (*4, 11–13*). However, it has also been observed that at low doses of ionizing radiation, no detectable *de novo* DSBs are produced (*11*), and in mutant cells defective in non-homologous end joining low-levels of DSBs are generated postirradiation (*12*). Recent results suggest that during repair of clustered damages the cells have mechanisms whereby the formation of *de novo* DSBs

---

[1] Dedicated to the memory of Betsy Sutherland, my scientific mentor and coauthor who died October 7, 2009 (*Radiat. Res. 173*, 401–402, 2010).

[2] Address for correspondence: Biology Department, Brookhaven National Laboratory, 50 Bell Ave., Upton, New York 11973; e-mail: keszenman@bnl.gov.

can be avoided or very rapidly resolved. These mechanisms include not only the base excision repair pathway but also accurate and inaccurate repair through the non-homologous end-joining pathway as well as Ku80-independent processes such as microhomology-mediated end joining and single-strand annealing (9, 14–16). The induction of these highly complex DNA damages in cells enhances the probability of incorrect or incomplete repair and thus may constitute a source of genomic instability involved in processes such as cell death, mutagenesis, carcinogenesis and aging.

Previous studies on the genome of bacteriophage T7, a 40-kbp DNA, indicate that the absolute yields of clustered DNA damages depend on the DNA environment and on the incident radiation. Irradiation of T7 DNA in a radioquenching solution induces significantly lower frequencies of clusters than in a non-radioquenching milieu. In addition, the damage spectrum—the relative levels of the different cluster types—are different in both conditions, exhibiting a significant decrease in the level of abasic clusters in relation to that of DSBs (5, 17). Using the same biological system, Hada and Sutherland (18) showed that in non-radioquenching conditions high-energy protons (1 GeV) produce DNA damage spectra similar to those of other high energy (HZE) particles but unlike those of photons of similar LET.

Theoretical and experimental in vitro and in vivo studies demonstrate a direct dependence of the biological effects of densely ionizing radiations on LET as reflected by the increase in the relative biological effectiveness (RBE) with a peak in the LET range of 100 to 200 keV/μm (19–22). In apparent disagreement with these results, in DNA in solution and in Chinese hamster cells, the yields of different types of isolated as well as clustered DNA damages decreased as a function of increasing LET (18, 23). However, in these studies, the kinetic energy of the HZE-particle radiations used varied and the species of HZE ions increased in atomic number (Z). Both magnitudes, the kinetic energy and the Z of the charged particle, which are related to the LET, characterize the spatial distribution of energy deposition along the particle track (24), affecting the radial extent and level of the indirect and direct effects of radiation. Therefore, to study the LET dependence of the biological effects of densely ionizing radiation when the LET modification is related to changes in the ionization density along the track, we have determined the types and yields of clustered DNA damages induced by charged-particle beams of different Z and similar kinetic energy per nucleon. In addition, since the absolute and relative levels of clustered lesions depend on the DNA microenvironment, we examined the LET dependence of the clustered damage spectrum by irradiating DNA in solutions of different free radical scavenging capacity. Yeast chromosomal DNA embed-ded in agarose plugs in non-radioquenching or radio-quenching solutions was irradiated with charged-particle beams of 1 GeV protons (Z = 1), 1 GeV/nucleon oxygen (Z = 8), 980 MeV/nucleon titanium (Z = 22) and 968 MeV/nucleon iron (Z = 26). Pulsed-field gel electrophoresis (PFGE) and number average length analysis were used to quantify the frequencies of DNA clustered lesions. Whereas the yields of total DNA damages calculated per absorbed dose in Gy induced by charged-particle radiation in non-radioquenching buffer decreased with increasing LET, the yield of clustered lesions in DNA irradiated in radioquenching buffer exhibited minor variations. However, the total damage yields calculated per particle fluence increased with LET in both non-radioquenching and radioquenching conditions, indicating a higher efficiency per particle to induce DNA clustered damage. The yields of DSBs and non-DSBs varied with LET as did the clustered damage spectra. In non-radioquenching conditions, the DSBs accounted for more than half of the total damages independent of the LET. However, a slight increase in the ratio of formamidopyrimidine-DNA glycosylase (Fpg) to endonuclease IV (Nfo) cleavable clusters of damaged DNA was observed with increasing LET. On the other hand, in radioquenching conditions the levels of DSBs increased with LET but their percentages for all the charged-particle irradiations used were lower than those for the non-DSB clusters. The ratio of Fpg to Nfo clusters decreased with LET mainly due to the reduction of the Fpg cluster levels. Collectively, the data indicate that more than one mechanism is involved in the formation of the different types of clustered damages, with the effect of the DNA microenvironment being variable.

MATERIALS AND METHODS

Yeast Cells and Growth Conditions

The haploid wild-type yeast strains BY4742 (*MATα his3Δ1 leu2Δ0 lys2Δ0 ura3Δ0*, Euroscarf, Frankfurt, Germany) and YPH755 (*MATα ura3-52 lys2-801 ade2-101 his7 trp1Δ1 CFVII(RAD2. p.YPH149)* [(*CFVII (RAD2.d.YPH146.TRP1)*], ATCC 47058, American Type Culture Collection, Rockville, MD) were used. Yeast cell cultures were obtained by inoculation of an isolated single colony in YPD liquid nutrient medium [1% yeast extract (BD, Franklin Lakes, NJ), 2% bactopeptone (BD) and 2% glucose (Mallinckrodt Inc., St. Louis, MO)]. After 24 h at 28°C with aeration by shaking, an aliquot of the culture was inoculated into fresh YPD medium (dilution 1/1000). Cells were grown at 28°C with aeration by shaking to stationary phase (1.5 × 10⁸ cells/ml). Cell density was assessed microscopically by using a Neubauer chamber.

DNA Isolation

DNA was isolated and embedded in agarose plugs as described previously with some modifications (25). Yeast cells were harvested by centrifugation and washed once with phosphate-buffered saline (PBS) and twice with 50 m*M* EDTA (pH 7.5). The cells were then resuspended in the volume ratio of 3:1 of 50 m*M* EDTA and Solution

	Proton	Oxygen	Titanium	Iron
Atomic number (Z)	1	8	22	26
Atomic mass number (A)	1	16	48	56
Energy (MeV/nucleon)	1000	1000	980	968
LET (keV/μm)	0.22	14	108	151
Dose rate (Gy/min)	0.6–1.3	0.3–2.5	1.2–10.6	0.7–12.1

I at a concentration of 1×10^9 cells/ml [Solution I: SEC buffer (1 M sorbitol, 10 mM citric acid, 10 mM disodium phosphate, 100 mM EDTA) plus 3 mg/ml Lyticase (Sigma-Aldrich, St. Louis, MO)]. The cell suspension was mixed with an equal volume of 2% low-melting-point agarose (InCert, FMC, Rockland, ME) in 0.125 M EDTA (pH 7.5) at 42°C and distributed into a plug mold. All solutions used in DNA isolation that did not contain enzymes or detergents were bubbled with 100% argon gas for at least 15 min before use to avoid formation of additional DNA oxidative lesions (5, 26). Also, during DNA isolation all incubations were at temperatures of 37°C or less to diminish formation of DNA strand breaks at heat-labile sites (12, 26–28) and with minimal mechanical shear to prevent fragmentation of high-molecular-weight DNA (29). The solidified plugs were transferred into 5-ml plastic tubes and incubated with Solution II at 37°C for 2 h [Solution II: 0.5 M EDTA (pH 8.0), 0.01 M Tris-HCl (pH 8.0) and 10 μg/ml RNase (Sigma-Aldrich, St. Louis, MO)]. After spheroplast induction, the agarose plugs were placed in lysis solution III consisting of 0.5 M EDTA, 0.01 M Tris-HCl, 1% n-lauroylsarcosine and 1 mg/ml Proteinase K (Roche Molecular Biochemicals, Indianapolis, IN) and incubated at 37°C for 36 h. Digested plugs were rinsed twice with Solution IV [10 mM Tris-HCl (pH 7.5), 10 mM EDTA and 1 mM phenylmethylsulfonylfluoride (PMSF)] at 4°C for 1 h. The agarose plugs were then rinsed several times and stored in Tris-EDTA buffer (TE) [10 mM Tris-HCl (pH 7.5) and 1 mM EDTA] at 4°C. The DNA content per plug was estimated from the cell concentration of the cell suspension.

Preirradiation Treatments and Ion-Beam Irradiation

Agarose plugs containing yeast DNA were washed several times with cold solutions of 10 mM KPO$_4$ (pH 7.4) as non-radioquenching solution and with 10 mM Tris-HCl (pH 8.0) (radioquenching solution) during 48 h prior to irradiations and kept at 4°C. Plastic tubes containing yeast DNA plugs in 3-ml buffer solutions were irradiated with ion beams at the NASA Space Radiation Laboratory (NSRL, Brookhaven National Laboratory). Tubes were placed in a single line perpendicular to the axis of the beam, and for each dose, samples in cold 10 mM KPO$_4$ and in 10 mM Tris were exposed to radiation at room temperature. The Physics Dosimetry group at NSRL carried out the dosimetry and provided the information about the ion-beam characteristics. The radiation species, energies, LET values and dose rates of the ion beams used are shown in Table 1. Immediately after irradiation, either the KPO$_4$ or Tris buffer solutions were completely removed from the tubes and replaced by 4 ml TE. Plugs were washed three times with 4 ml cold TE and kept at 4°C.

Radiation-Induced Double-Strand Breaks, Abasic Sites and Oxidized Purine Clusters in Yeast DNA

For lesion-specific enzyme treatment, each DNA plug was divided and each half was transferred to 70 mM Hepes/KOH, pH 7.6, 100 mM KCl, 1 mM EDTA, pH 7.6, and then to the same buffer with 1 mM dithiothreitol (DTT) and 10 mg/ml bovine serum albumin (BSA) at 4°C. Then one half plug was incubated at 37°C for 20 h with buffer alone while the other half was treated with sufficient quantities of homogeneous enzyme protein to cleave at all cluster sites for that enzyme. E. coli Fpg protein and E. coli Nfo protein (Endonuclease IV) were prepared in this laboratory as described previously (7, 30). For a half-plug containing 750 ng yeast DNA, this corresponded to 60 ng of E. coli Fpg protein and 60 ng of E. coli Nfo protein (Endonuclease IV). Substrates for Fpg protein include 4,6-diamino-5-formamidopyrimidine (FapyAde) and 2,6-diamino-5-formamidopyrimidine (FapyGua), 2,6-diamino-4-hydroxy-5-N-methylformamidopyrimidine (MethylFapyGua), 8-oxo-7, 8-dihydro-2'-deoxyguanosine (8-oxodGuo), some abasic sites, C8-oxoadenine and, to a lesser extent, other modified purines (31–34). Fpg protein also cleaves some pyrimidine derivatives in synthetic oligonucleotides (33, 35) but fails to release these bases in irradiated DNA. Nfo protein recognizes and cleaves several types of abasic sites including regular as well as oxidized abasic sites and anoxic radiolysis DNA product α-deoxyadenosine (36, 37). Using oligonucleotide substrates, it was shown that Nfo protein has DNA-glycosylase activity recognizing and incising oxidatively damaged pyrimidines (38). After digestion was complete, plugs were washed with L buffer [20 mM NaCl, 0.1 M EDTA and 10 mM Tris-HCl (pH 8.0)]. Traces of Nfo or Fpg protein were removed by addition of 1 mg/ml proteinase K and 1% sarcosyl in L buffer and incubation at 37°C overnight. Then plugs were rinsed and stored in TE at 4°C. Companion plug samples for determination of radiation-induced DSBs were kept in TE at 4°C.

Measurement of Clustered DNA Damage

Control and irradiated samples were electrophoresed along with molecular length standards (DNA from bacteriophage λ, a HindIII digest of bacteriophage λ and Saccharomyces cerevisiae chromosomes of the strain YPH755) using neutral pulsed-field gel electrophoresis (Gene Navigator, GE Healthcare). Samples were electrophoresed in 1% Sea Kem agarose (BioWhittaker Molecular Applications, Rockland, ME) in 0.5× TBE (1× TBE is 90 mM Tris borate, 2 mM EDTA, pH 7.8) for 20 h using 0.5× TBE as electrophoresis buffer and a linearly ramping pulsing regime from 0 s to 180 s, at 165 V, 9°C. Gels were stained with ethidium bromide (1 μg/ml) in double-distilled water and destained overnight, and a quantitative electronic image was obtained as described (39). A DNA dispersion curve was determined from an analytical mobility function based on the DNA length standards mentioned above. From the DNA distribution of each experimental sample, the number average lengths (L_n) were computed and the frequencies of DSBs, oxypurine clusters and abasic clusters were calculated as described (2, 40). In brief, the frequency of DSBs, ϕ_{DSB}, for each radiation dose was calculated from the equation

$$\phi_{DSB} = 1/L_n(\text{irradiated}) - 1/L_n(\text{no radiation}), \quad (1)$$

where $1/L_n$(irradiated) and $1/L_n$(no radiation), are the reciprocals of the number average lengths of irradiated and unirradiated samples. The frequencies of clusters ϕ_C (oxypurine or abasic clusters) at each radiation dose D, ascertained by treatment of half of the sample with the lesion-specific enzyme and the other half incubated without enzyme, were calculated from the equation

$$\phi_C = 1/L_n(\text{irradiated}_D + \text{enzyme}) - 1/L_n(\text{irradiated}_D - \text{enzyme}), \quad (2)$$

where $1/L_n$(irradiated$_D$ + enzyme) and $1/L_n$(irradiated$_D$ − enzyme) are reciprocals of number average lengths of sample pairs irradiated with dose D, with and without enzyme, where the enzymes are Fpg and Nfo enzymes, respectively.

Data from at least three reproducible experiments are given in the figures, and standard errors of the means were plotted. Best-fitting regression lines were fitted to the data with SigmaPlot Version 6 and the method of least squares. Estimates of the intercept and the slope were obtained for each line from the SigmaPlot program. The 95% confidence intervals are shown as dotted belts to indicate the accuracy of the estimate of Y for each value of X over the X axis. Least-squares

regression lines for the non-radioquenching and the radioquenching data were fitted separately with the SigmaPlot program. The hypothesis that the slope of each line is equal to zero was tested with Snedecor's F ratio and an analysis of variance.

RESULTS

### Standardization of Clustered DNA Damage Determinations

The radiation induction of clustered DNA damages can be detected and quantified using PFGE, electronic imaging and number average length analysis (40). To evaluate the effects of radiation dose, particle fluence and DNA microenvironment on DNA damage, we used chromosomal yeast DNA as the biological system and PFGE, which allows the separation of linear DNA molecules in the megabase-pair size range according to their length and causes minimal disruption of DNA through shearing (28, 29). Yeast cells from stationary-phase cultures consisting mainly of G_1 cells were used to avoid the presence of chromosomes with replicating structures that may not enter the gel from the plug. Since the migration distance from the well into the agarose gel depends on the size (length) of the linear chromosomal molecule, the DNA fragmentation due to DSBs is observed as an increase of the number of molecules of smaller length that show further migration. Figure 1 shows a typical electronic image of a neutral agarose gel for detecting DSBs induced by exposure of yeast DNA in a non-radioscavenging milieu to increasing doses of iron ions (968 MeV/nucleon). Lane 3 corresponds to the chromosome separation of the control (0 Gy). In the successive lanes, from 4 to 8, a decrease in the intensity of the individual chromosomal bands was observed along with a corresponding increase of the smear, which indicates the magnitude of DNA fragmentation. The DNA profile of the DNA length standards is shown in Fig. 2A, where M1 corresponds to *S. cerevisiae* (lanes 1 and 9) and M2 is DNA from bacteriophage λ and a *Hin*dIII digest of bacteriophage λ (lanes 2 and 10). Based on these DNA standards, a dispersion curve was generated to relate the DNA length to the mobility in the gel (Fig. 2B). The changes in the DNA profiles as the radiation dose increases (corresponding to lanes 3, 5, 6 and 7) are presented in Fig. 2C. Compared to the control, at each dose, the population of molecules of greater length decreased with the corresponding increase in the number of molecules with shorter lengths and therefore with higher gel mobility. From the DNA distribution of each experimental sample the number average lengths (L_n) were computed and the frequencies of DSBs were calculated according to Eq. (1).

To assess non-DSBs clusters, the samples were treated in addition with a lesion-specific enzyme prior to electrophoresis (2, 40). A two-site cluster can be constituted either from a single-strand break opposed to a specific
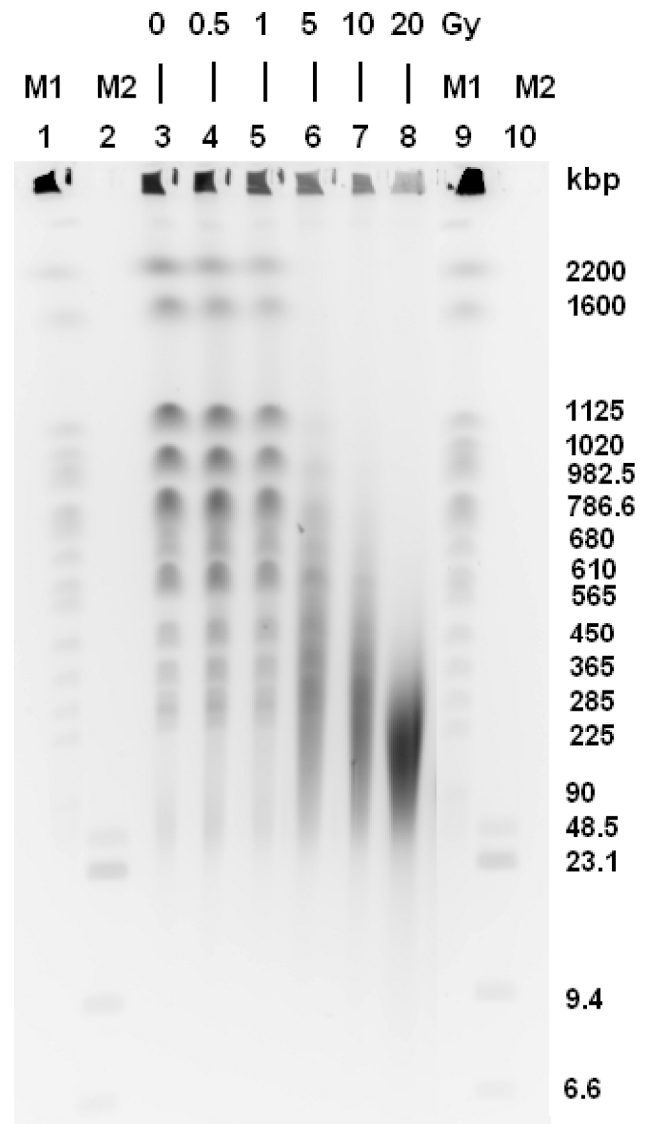
FIG. 1. Electronic image of a neutral agarose gel for analysis of DSBs induced in yeast DNA in 10 mM phosphate buffer by exposure to 968 MeV/nucleon $^{56}Fe^{26}$ particles. Lane 3: unirradiated sample; lanes 4–8: increasing doses (D) of iron ions ($0.5 \leq D \leq 20$ Gy). DNA length standards M1 is *S. cerevisiae* (lanes 1and 9), M2 is DNA from bacteriophage λ and a *Hin*dIII digest of bacteriophage λ (lanes 2 and 10).

enzyme site or by two opposing enzyme recognized sites. In both cases, after enzyme cleavage the final result is the generation of a DSB detectable by PFGE. We have used Fpg protein to detect mainly oxypurine clusters and Nfo protein for principally abasic clusters. Due to the variety of substrates for both enzymes, clusters recognized and cleaved by Fpg protein are designated as Fpg clusters and the ones recognized and cleaved by Nfo protein are termed as Nfo clusters. To determine the optimum amount of Fpg and Nfo enzymes needed in our megabasepair DNA experimental system, the titration curves for each enzyme were obtained using DNA samples exposed to 0 or 5 Gy of 1 GeV protons.
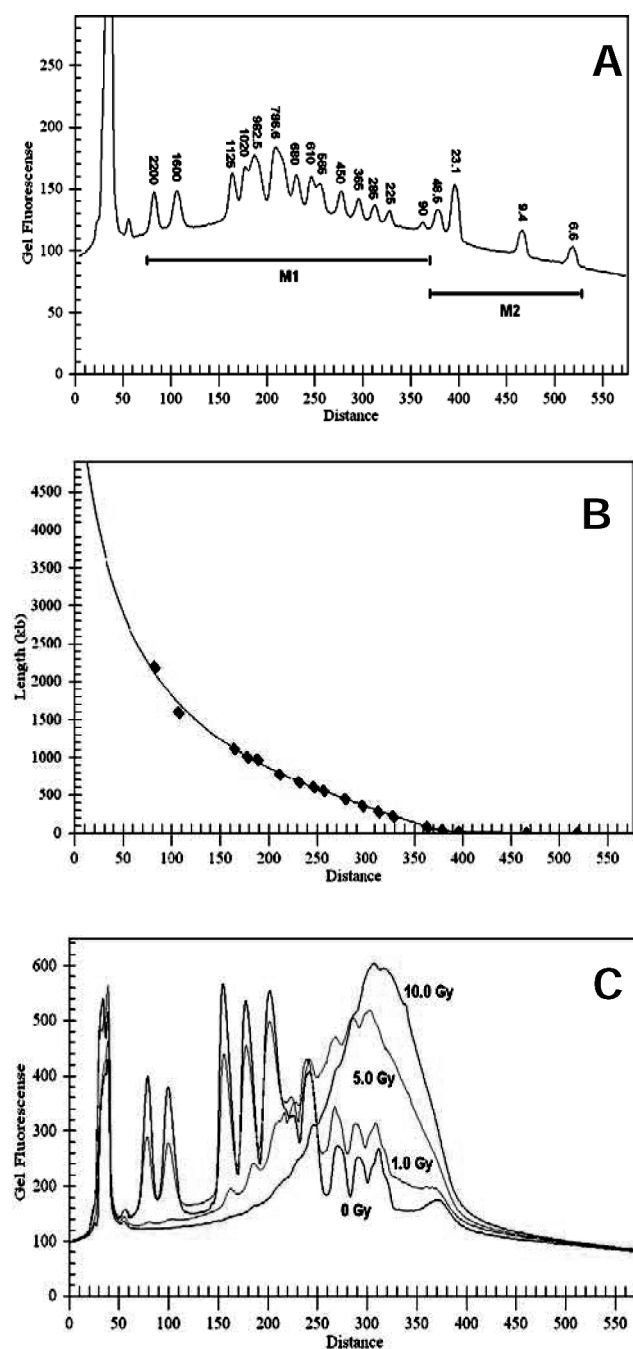
FIG. 2. Panel A: Ethidium-bound DNA fluorescence profile of the DNA length standards M1 (*S. cerevisiae*) and M2 (bacteriophage λ and a *Hind*III digest of bacteriophage λ). Panel B: Since each peak corresponds to a single mean DNA length in kbp, these data were used to generate the continuous dispersion curve that relates the DNA length to the mobility in the gel required for the number average length analysis. Panel C: DNA fluorescence profiles of the yeast DNA samples exposed to increasing doses of 968 MeV/nucleon [56]Fe[26] ions. Each profile corresponds to the DNA in lanes 3, 5 and 7 (0, 1, 5 and 10 Gy, respectively) shown in Fig. 1.

Figure 3 shows that for both enzymes, Fpg (panel A) and Nfo (panel B), approximately 60 ng of protein per 750 ng of yeast DNA was sufficient to detect the maximum amount of the corresponding clusters, with little cleavage of unirradiated DNA. Therefore, this amount was chosen as optimal for both enzymes for further experiments. The electronic image of an agarose gel for Nfo clusters determination in samples irradiated in 10 mM phosphate buffer with increasing doses of iron ions is presented in Fig. 3C. Unirradiated DNA treated with Nfo protein (lane 4) shows very little DNA fragmentation compared with the untreated sample (lane 3), indicating a low level of endogenous Nfo clusters. Within a given dose, the radiation induction of Nfo clusters was observed as an increase in the population of molecules of shorter length in the enzyme-treated sample compared to the non-enzyme-treated sample (for example, compare lanes 9 and 10). From the dispersion curve obtained from the length standards M1 and M2 and the DNA distribution of each lane, the number of average length was determined, and the frequency of Nfo clusters at each radiation dose was calculated according to Eq. (2).
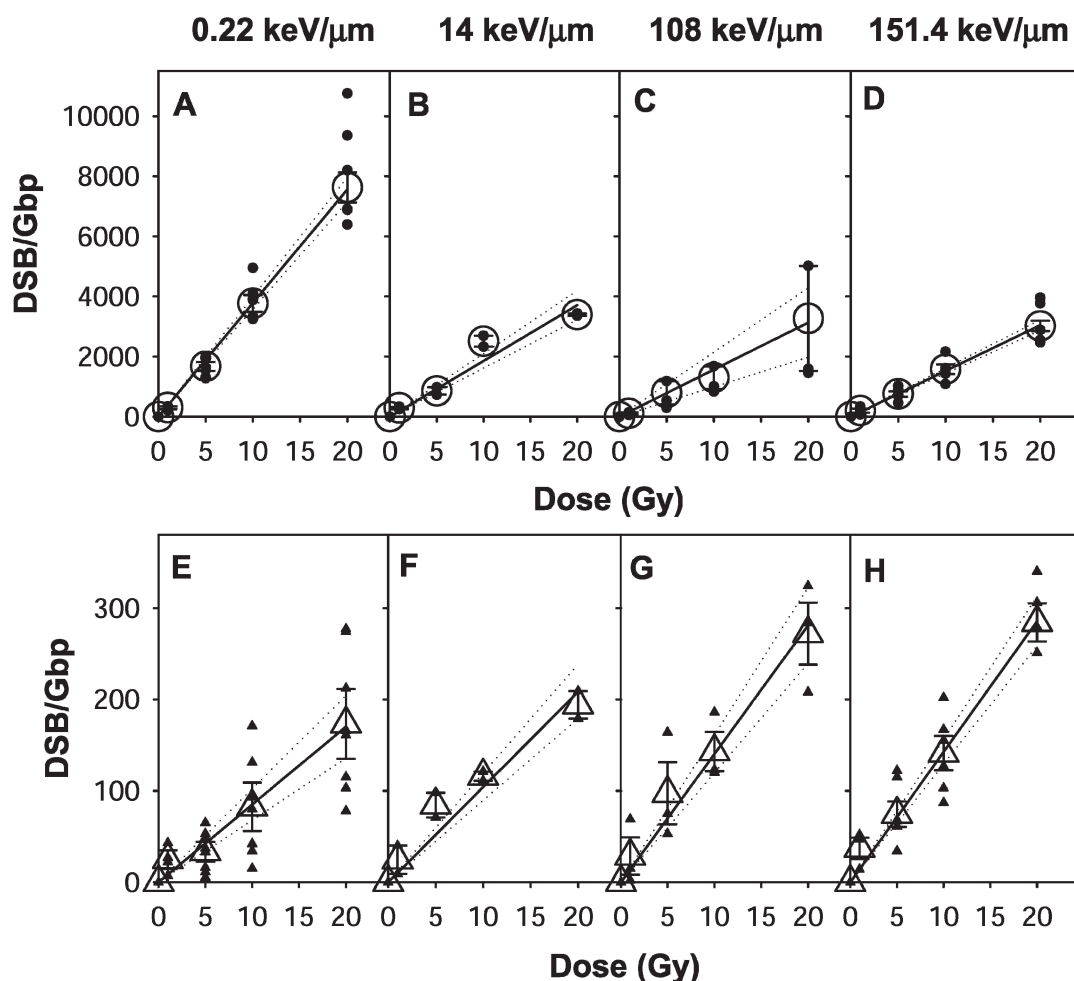
Dose Response of Clustered DNA Damages and Effect of DNA Microenvironment

To study the influence of the LET in the production of bistranded clusters, yeast DNA embedded in agarose plugs was irradiated with beams of particles with similar kinetic energy (968 to 1000 MeV/nucleon) but different atomic number (Z). The dose–response curves for DSB induction by exposure to protons and oxygen, titanium and iron ions in non-radioquenching conditions (DNA plugs suspended in 10 mM phosphate buffer) are shown in Fig. 4A–D, respectively. Protons, the ion species of the lowest LET (0.22 keV/μm) used in this study, induced the highest frequencies of DSBs (Fig. 4A). The other ion beams used showed significantly lower DSB frequencies than protons (Fig. 4B–D). A slight decrease in the frequencies with increasing LET was observed among these three charged particles despite the large difference in the LETs. When DNA plugs were irradiated in radioquenching conditions (10 mM Tris), the absolute frequencies of DSBs increased with increasing LET (Fig. 4E–H). DSBs frequencies induced by the four charged particles were lower than those in non-radioquenching conditions, in agreement with previous results that show lower levels of clustered DNA damage induced by ionizing radiation in presence of scavengers (*2, 17, 41*). In our experimental system, the frequencies of induced DSBs in radioquenching conditions decreased approximately 44-fold for protons (Fig. 4E), 18-fold for oxygen ions (Fig. 4F), and 10-fold for both titanium and iron ions (Fig. 4G and H, respectively) compared to the levels observed in non-radioquenching conditions.

We next determined the dose responses for the induction of Fpg and Nfo clusters by protons and oxygen, titanium and iron ions (Figs. 5 and 6, respec-
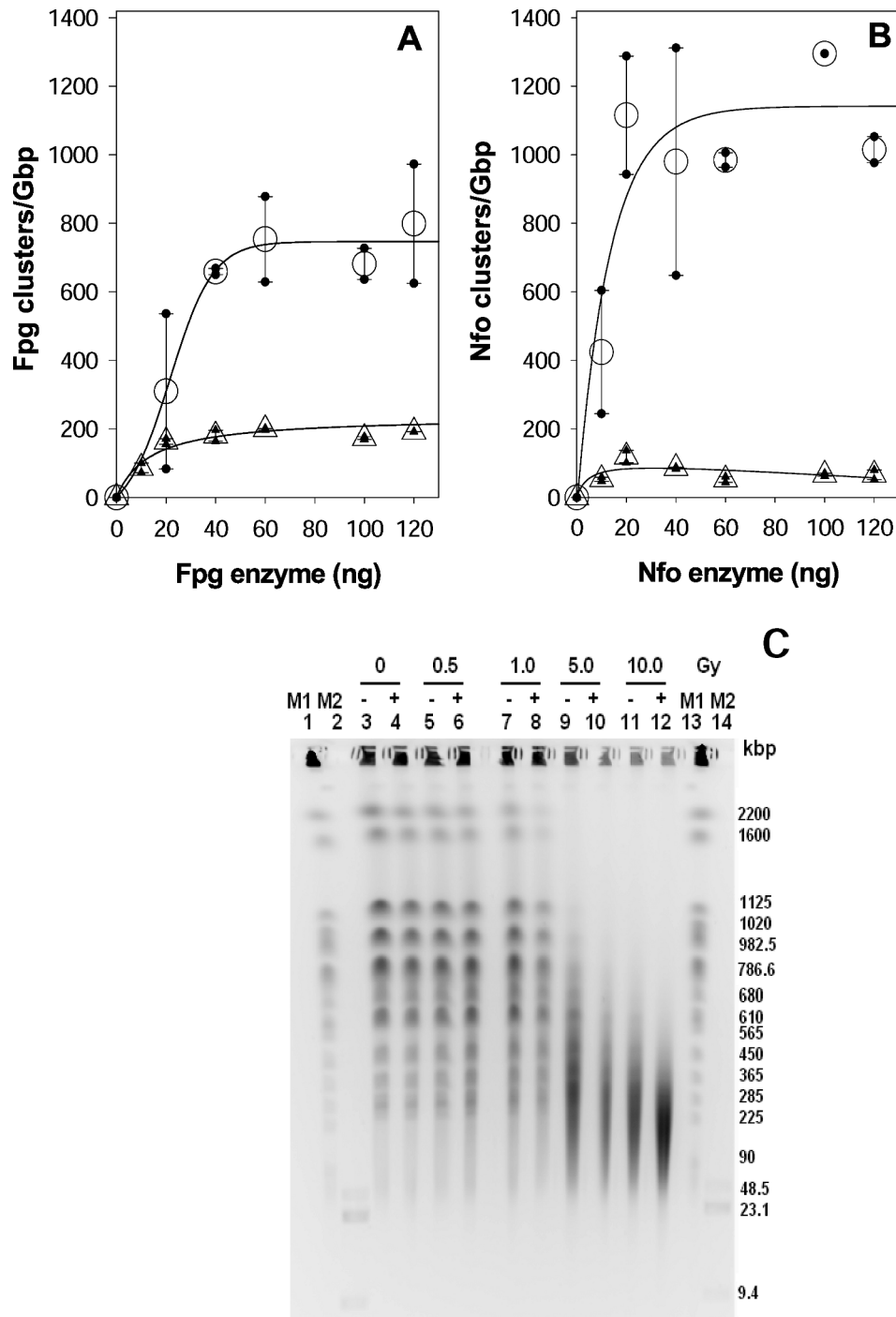
FIG. 3. Titration of yeast DNA with Fpg (panel A) or Nfo (panel B) enzymes to assess the amount of Fpg and Nfo proteins required for optimal cleavage. DNA in agarose plugs in 10 mM phosphate buffer were exposed to 1 GeV proton beams at 0 Gy (triangles) or 5 Gy (circles). After irradiation, half-plugs containing 750 ng yeast DNA were treated with increasing amounts of Fpg or Nfo proteins under appropriate reaction conditions (see the Materials and Methods). Solid symbols correspond to individual data points and open symbols to averages of two experiments. The error bars correspond to the standard errors of the means. Sites per Gbp were calculated as described in the Materials and Methods. Panel C: Electronic image of a neutral agarose gel for determination of Nfo DNA clustered damage in yeast DNA in 10 mM phosphate buffer irradiated with increasing doses of 968 MeV/nucleon $^{56}Fe^{26}$ ions. At each radiation dose, the Nfo protein treatment of part of the DNA samples (+enzyme) led to the formation of additional DSBs, due to cleavage at the sites of clusters, compared with the untreated part of the samples (–enzyme). Lanes 3 and 4: 0 Gy; 5 and 6: 0.5 Gy; 7 and 8: 1 Gy; 9 and 10: 5 Gy: 11 and 12 10 Gy. DNA length standards were M1 corresponding to *S. cerevisiae* (lanes 1 and 13) and M2 is DNA from bacteriophage λ and a *Hin*dIII digest of bacteriophage λ (lanes 2 and 14).

FIG. 4. Dose–response curves for DSB induction by exposure to charged particles of different atomic number (Z) of yeast DNA in 10 mM phosphate buffer (upper panels) or in 10 mM Tris (bottom panels). Panels A and E show the effect of 1 GeV protons, panels B and F of 1 GeV/nucleon $^{16}O^8$ ions, panels C and G of 980 MeV/nucleon $^{48}Ti^{22}$ ions, and panels D and H of 968 MeV/nucleon $^{56}Fe^{26}$ ions. LET values of each charged-particle beam are indicated on top of the upper panels. Solid symbols correspond to individual data points and open symbols to averages of at least two independent irradiation experiments except for $^{16}O^8$ ions. The error bars correspond to the standard errors of the means, and 95% confidence intervals are shown by dotted lines.

tively). As expected, the levels of clusters at 0 Gy (endogenous clusters) in the samples incubated in a radioquenching solution was two to three times lower than those in phosphate buffer. Also, as observed for DSBs, the frequencies of both Fpg and Nfo clusters were lower when irradiations were performed in Tris (bottom panels) than those in phosphate buffer (top panels). Five- to sevenfold fewer Fpg clusters were induced by protons and titanium and iron ions in Tris buffer (Fig. 5). However, the level of reduction of Nfo clusters was more variable (Fig. 6). In both irradiation conditions, Fpg clusters frequencies decreased with increasing LET (Fig. 5). In the case of Nfo clusters, the highest frequencies were observed for proton irradiation in phosphate buffer (Fig. 6A), while the other charged particles induced significantly lower levels of clusters (Fig. 6B–D). In radioquenching conditions, the Nfo

cluster induction was similar by all the radiation species tested (Fig. 6E–H).

Yields and Spectra of Clustered DNA Damages: LET Dependence

To further evaluate the influence of the LET on the induction of DNA clustered damages, we determined the yields of clusters/Gbp Gy^{-1} and the spectra of damages for each charged particle. The log-log plots of the cluster yields as a function of the LET values show a frank decrease in clusters yields with increasing LET when DNA was irradiated in non-radioquenching phosphate buffer (Fig. 7A–C, upper plots), whereas in the presence of a scavenger such as Tris, the yield slope depended on the type of cluster (bottom plots). In fact, the DSB yields increased significantly with increasing
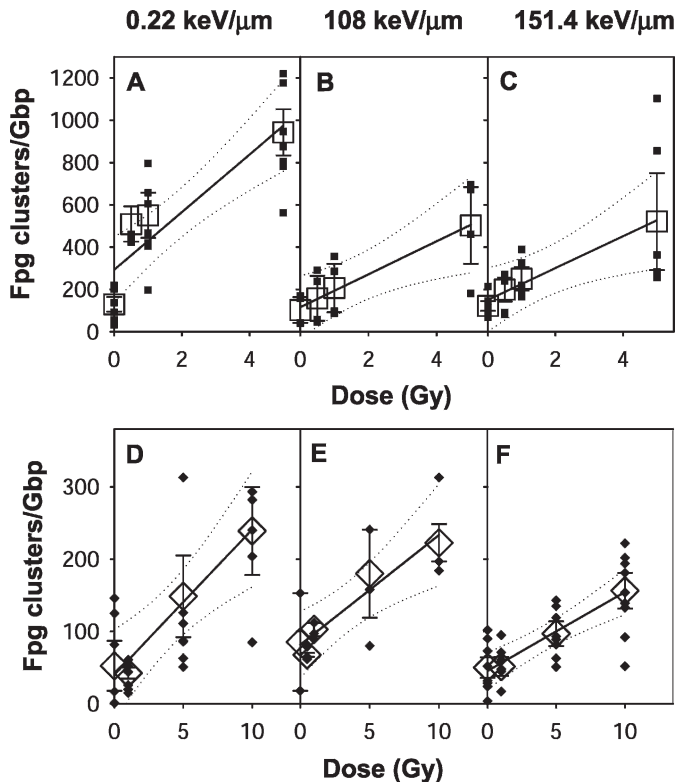
FIG. 5. Dose–response curves for Fpg clustered damage induction by exposure to charged particles of different atomic number (Z) of yeast DNA in 10 mM phosphate buffer (upper panels) or in 10 mM Tris (bottom panels). Panels A and D correspond to 1 GeV protons, panels B and E to 980 MeV/nucleon ^{48}Ti^{22} ions, and panels C and F to 968 MeV/nucleon ^{56}Fe^{26} ions. LET values of each charged-particle beam are indicated on top of the upper panels. Solid symbols correspond to individual data points and open symbols to averages of at least two independent irradiation experiments. The error bars correspond to the standard errors of the means, and 95% confidence intervals are shown by dotted lines.

LET (Fig. 7A). The Fpg clusters showed a decrease (Fig. 7B), although the small number of points does not permit us to draw a significant conclusion and the Nfo cluster yields exhibited little variation (Fig. 7C). The total DNA damage yield induced by each charged particle per unit of absorbed dose in Gy, calculated as the sum of the yields of the assessed classes of clustered damages, decreased as a function of LET in non-radioquenching conditions and showed little variation in a radioquenching environment (Table 2). Since the particle fluences per Gy n(r) in particles/cm^2 Gy^{-1} calculated according to the relationship for water of n(r) = 6.242 × 10^8/LET (keV/μm) for the four charged particles decrease significantly with the LET, we calculated the clustered yields per particle fluence. In both irradiation conditions, the total yields increased with LET (Table 2), showing the higher efficiency of the production of DNA damage by charged particles of high LET. To assess the differential contribution to the total production of DNA damages of each class of clustered damage, the percentages of each type of lesion induced

by protons and titanium and iron ions were calculated from the data shown in Fig. 7. Table 3 displays the percentages of clustered damages in both non-radio-quenching and radioquenching milieu. While in non-radioquenching conditions, the DSBs accounted for approximately 50% of clustered DNA damages for the three charged particles, in radioquenching conditions the percentage of DSBs increased with increasing LET. For oxygen ions, the yield of DSBs was higher than that for Nfo clusters (Fig. 7). Therefore, these data indicate that in DNA irradiated in non-radioquenching conditions the charged particles induce a similar spectrum of damages considered as the levels of DSBs relative to non-DSB clusters. The percentages of Nfo clusters were the lowest of all the damage classes except in the case of proton irradiation in phosphate buffer. In DNA irradiated in Tris, the percentages of Fpg clusters decreased with increasing LET at levels comparable to the increase of DSBs.

DISCUSSION

Ionizing radiation induces bistranded clustered DNA damages including DSBs, oxidized bases and abasic sites in DNA in solution as well as in living cells. The cellular processing of these diverse DNA lesions is thought to be complex due to the enhanced probability of generation of DSBs as repair intermediates, persistence of non-repaired and misrepaired clusters as well as delayed repair, which in turn increases the probability of lethality and mutagenesis. The occurrence of any of these damage processing events depends on the types, level and spatial distribution of clustered DNA damages, and thus these parameters constitute key factors in the determination of their biological consequences (4, 9–12, 16, 42). To determine different types of clustered DNA damages, we have used PFGE and number average length analysis (Figs. 1–3).

Consistent with previous experimental and biophysical modeling studies (41, 43), our data indicated that the types and yields of clustered DNA damages depend on the DNA environment and on the quality and quantity of the incident radiation. A contributor to DNA damage induced by ionizing radiation is the indirect effect produced by the ionization of water, which results in the generation of highly reactive oxygen species (ROS) such as ·OH. Several reports have shown an inverse relationship between the level of DNA clusters and the free radical scavenging capacity of DNA environment (2, 17, 41, 44). In agreement with these results, the absolute frequencies of both DSBs and non-DSB clusters induced by the four charged-particle beams used in this study were significantly lower when DNA was irradiated in radioquenching conditions (10 mM Tris) than in a non-radioquenching solution (10 mM KPO$_4$) (Figs. 4–6 and Table 2). The incubation of DNA
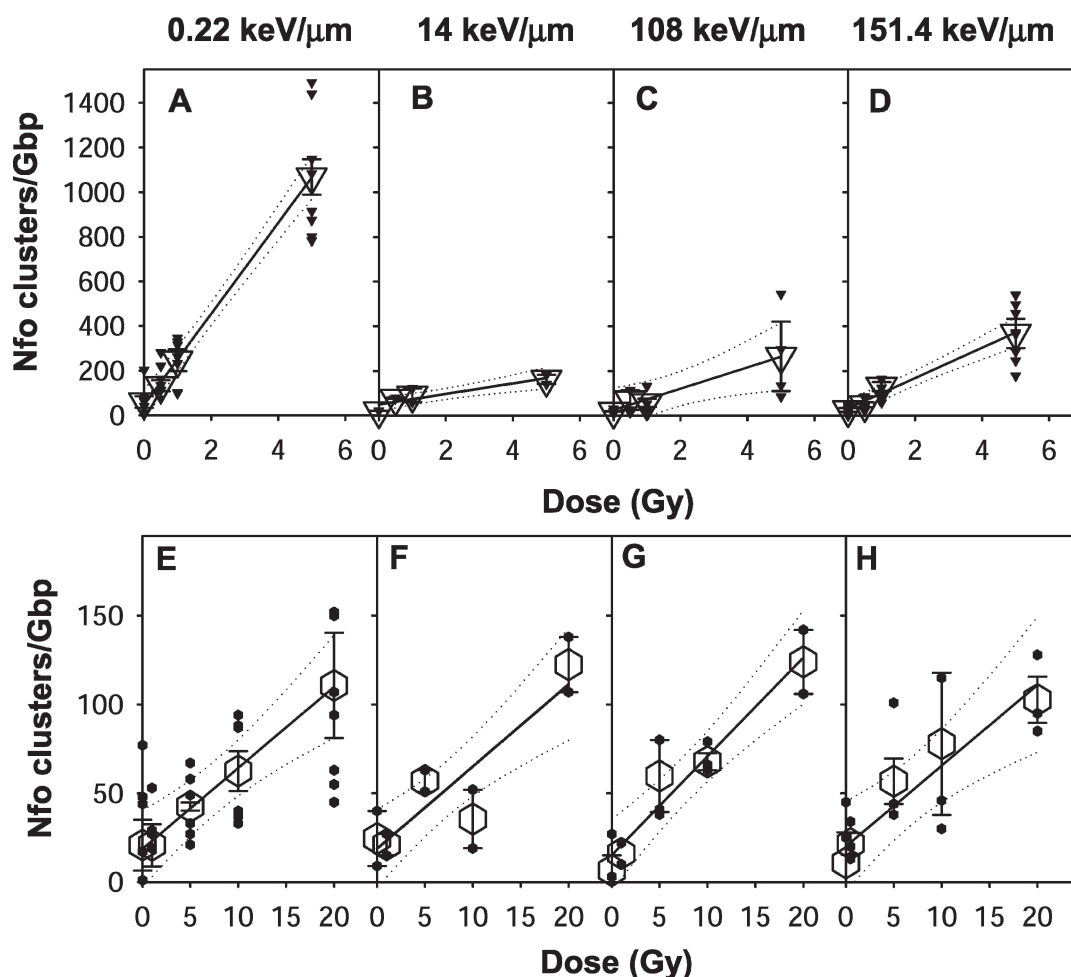
FIG. 6. Dose–response curves for Nfo clustered damage induction by exposure to charged particles of different atomic number (Z) of yeast DNA in 10 mM phosphate buffer (upper panels) or in 10 mM Tris (bottom panels). Panels A and E show the effect of 1 GeV protons, panels B and F of 1 GeV/nucleon $^{16}O^8$ ions, panels C and G of 980 MeV/nucleon $^{48}Ti^{22}$ ions, and panels D and H of 968 MeV/nucleon $^{56}Fe^{26}$ ions. LET values of each charged-particle beam are indicated on top of the upper panels. Solid symbols correspond to individual data points and open symbols to averages of at least two independent irradiation experiments except for $^{16}O^8$ ions. The error bars correspond to the standard errors of the means, and 95% confidence intervals are shown by dotted lines.

samples in the presence of a scavenger such as Tris buffer reduced the levels of endogenous Nfo and Fpg clusters two to three times compared to the levels observed in phosphate buffer (Figs. 5 and 6). These data thus clearly show that the levels of free radicals in the environment surrounding the DNA are important in the induction of clustered damages.

An important determinant of the stochastic biological events induced by the deposition of energy from charged-particle beams, which leads to ionization and excitation processes, is the track structure. The spatial distribution of the energy deposition is defined by the track of the primary ion (core) and the energy distribution of the secondary electrons (δ rays) that extends over distance from the track center (penumbra). The radial energy distribution around the track is characterized by the atomic number, Z, of the particle

and the ion kinetic energy per nucleon. While Z directly affects the level of ionization density along the track, the radial extent of the energy distribution is related to the kinetic energy of the ion. Both magnitudes are related to the radiation parameter LET, used as a measure of average energy deposition per unit distance along the track (24). When the energy per nucleon is constant, the maximum radial range of the secondary electrons of all ion beams is similar and the LET therefore reflects the ionization density of the ion track. In non-radioquenching conditions, our results show that the frequencies of the three types of clustered DNA damages—DSBs, Fpg and Nfo clusters—decreased as a function of absorbed dose as the LET of the radiation species increased (Figs. 4–6, top panels, Table 2). These results are in agreement with previous results obtained in T7 DNA irradiated in a non-radioquenching aqueous solution.
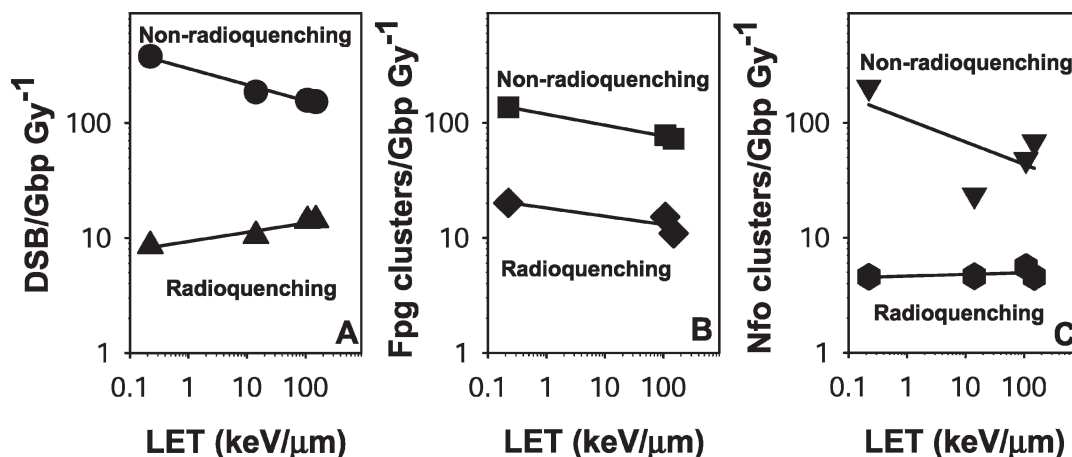
FIG. 7. Clustered DNA damages yields, calculated from the dose–response functions shown in Figs. 4–6, as a function of LET (keV/μm) in non-radioquenching 10 mM phosphate buffer (upper plots) and radioquenching 10 mM Tris (bottom plots) solutions for 1 GeV protons (LET: 0.22 keV/μm), 1 GeV/nucleon $^{16}O^8$ ions (LET: 14 keV/μm), 980 MeV/nucleon $^{48}Ti^{22}$ ions (LET: 108 keV/μm), and 968 MeV/nucleon $^{56}Fe^{26}$ ions (LET: 151 keV/μm). Panel A: DSBs; panel B: Fpg clusters; panel C: Nfo clusters.

However, the kinetic energy of the HZE-particle radiations used in those studies (18) and thus the radial extent of free radical formation varied. Since in DNA irradiated in non-radioquenching solution the indirect effect of radiation through the formation of ROS is very important, the decrease of the clustered damages yields as the LET increased could be attributed to the reduced availability of free radicals in the solution surrounding the DNA. In fact, it has been shown that as the LET increases, the ROS density increases along the ion track; however, the occurrence of intratrack radical recombination events leads to a decrease of the net yield of ROS. Also, the radicals formed by the δ rays close to the track axis can be enveloped by the ROS diffused from the core and may be involved in the inactivating recombination processes of free radicals (45–47). In addition, the observed decrease in the base damage cluster yields could be the result of an underestimation of the actual yields due to limitations of the Fpg and Nfo enzymatic assays used. In fact, multiple close base damages within a cluster may impair the recognition, binding and cleavage by these enzymes of some of the base damage

sites, thus preventing the formation of single-strand breaks.

Besides the observed lower frequencies of both DSBs and non-DSBs clusters induced by the charged-particle beams when DNA was irradiated in conditions mimicking the intracellular milieu, the frequencies of the different types of clustered damages as a function of the absorbed dose varied with increasing LET. As shown in the bottom panels of Figs. 4–6, the frequencies of DSBs increased with LET, the Fpg clusters frequencies decreased, and the Nfo cluster exhibited minor variations (Fig. 7). These data are in agreement with those of Kiefer et al. (48), who showed in diploid yeast cells irradiated with charged particles that the DNA breakage increases with increasing LET. However, in plasmid and lambda DNA irradiated with carbon and iron ions in 10 mM Tris solution, Terato et al. (23) found a decrease in the yields of DSBs, oxypyrimidine and oxypurine clusters leading to a decrease in the total clustered damage per Gy as LET increased. However, in the latter study, both parameters related to LET, kinetic energy and the Z of the beams, increased, affecting the

TABLE 2
Total DNA Clustered Damage Yields in Yeast DNA Calculated as a Function of Absorbed Dose and Fluence of Radiation with Charged Particles

	Total DNA damage yields				
	Per absorbed dose[a]			Per particle fluence[c]	
Charged particle	DNA in KPO₄	DNA in Tris	Particle fluence/Gy[b]	DNA in KPO₄	DNA in Tris
$^1H^1$	718.1	33.2	28.373	25.3	1.2
$^{16}O^8$	208.8	15.1	0.439	475.7	34.3
$^{48}Ti^{22}$	282.3	34.8	0.058	4866.4	600.0
$^{56}Fe^{26}$	295.5	29.5	0.042	7035.2	708.3

[a] Yield of clusters Gbp Gy⁻¹.
[b] Particle fluence in 10⁸ particles cm⁻².
[c] Yield of clusters Gbp/10⁸ particles cm⁻².

TABLE 3
Percentage of Clustered DNA Damages Induced in Yeast DNA by Radiation with Charged Particles

| | Percentage of clustered DNA damages | | | | | |
| | DNA in KPO$_4$ | | | DNA in Tris | | |
Clustered damage	^{1}H^1 1 GeV	^{48}Ti^{22} 980 MeV	^{56}Fe^{26} 968 MeV	^{1}H^1 1 GeV	^{48}Ti^{22} 980 MeV	^{56}Fe^{26} 968 MeV
Double-strand breaks	52.6	55.5	51.5	25.7	40.3	48.0
Fpg clusters	19.0	27.6	25.5	60.6	43.7	36.7
Nfo clusters	28.4	16.9	23.0	13.7	16.0	15.3

levels of ROS that react effectively with DNA. Using fully hydrated plasmid DNA in highly scavenging conditions to study the direct effects of ^{4}He^{2+} ion beams, Urushibara *et al.* (*49*) showed that with increasing LET the yields of DSBs increased whereas the yields of base lesions per Gy (Fpg and Nth recognized oxypurines and oxypyrimidines, respectively) decreased, resulting in an increase of the total clustered damage yields. Since the higher LET values were related to lower kinetic energies of the ^{4}He^{2+} ion beams, the radial extent from the ion track of the indirect effect was also lower. In the present work using ion beams of the same kinetic energy and different *Z*, the resulting total DNA damage yield induced per unit of absorbed dose in Gy showed little variation with the LET when DNA was irradiated in a radioquenching environment (Table 2). As mentioned above, an underestimation of the actual base damage yields due to limitations of the enzymatic assays used cannot be ignored in the determination of the resulting total damage yields. However, it should also be taken into account that at equal doses of ion beams of the same kinetic energy and different *Z* as the LET increases the number of particles/cm^2 or fluence decreases (Table 2). Therefore, the total DNA damage yields calculated per particle fluence increased with increasing LET (Table 2), indicating a direct relationship between the LET and the levels of clustered damage induced.

Since the spectrum of DNA clustered damages is an important determinant of their structural complexity, which influences their biological consequences (*9–12, 50*), we determined the spectra of damages as a function of the LET (Fig. 7, Table 3). In non-radioquenching conditions, the DSBs accounted for more than half of total clustered damages independently of the LET of the charged particle. Except for 1 GeV protons, the levels of Fpg clusters induced by HZE particles were higher than the Nfo clusters. Moreover, the relative percentages of Fpg clusters increased with LET while the Nfo clusters decreased, leading to a slight increase in the ratio of both clusters as a function of LET, in accordance with previous observations (*18*). On the other hand, in yeast DNA irradiated in radioquenching milieu the spectrum of damages induced by three charged particles was different. Although the DSB levels increased with LET,

their percentages in all charged particles were lower than the non-DSB clusters. The ratio of Fpg clusters to Nfo clusters was above unity but decreased with increasing LET due to the decrease in the relative levels of Fpg clusters. These results indicate that the formation of the different types of clustered DNA damages induced by particle radiation involves more than one mechanism with variable relevance according to the DNA microenvironment. In non-radioquenching conditions, as the LET increases, the resulting clustered DNA damages most probably arise from the balance between their increased formation due to higher direct ionization of DNA and their reduced generation caused by lower yields of highly reactive radicals (e.g. ˙OH) due to intratrack recombination processes. In radioquenching conditions, the direct effect of radiation prevails, leading to an increase in DSBs as LET increases. Moreover, since the ROS generated are scavenged by Tris and also the diffusion of the ˙OH is limited, non-DSB clusters decrease, mainly due to the reduction in the oxypurine levels. These results suggest that as the LET of the charged-particle radiation increases, the DSBs become the main type of DNA damage, increasing the probability of immediate lethal cellular events. The non-DSB lesions such as oxidized bases and abasic sites in the proximity of DSBs would contribute to the complexity of the cluster damage, leading to enhanced mutagenesis and eventually delayed cell death. Therefore, due to the biological significance of relative levels of clustered damages, experiments are in progress to determine if the kinetic energy of the ion beam as determinant of the LET-produces LET dependent modifications of the damage spectra.

REFERENCES

1. F. A. Cucinotta and M. Durante, Cancer risk from exposure to galactic cosmic rays: implications for space exploration by human beings. *Lancet Oncol.* **7**, 431–435 (2006).

2. B. M. Sutherland, P. V. Bennett, O. Sidorkina and J. Laval, Clustered DNA damages induced in isolated DNA and in human cells by low doses of ionizing radiation. *Proc. Natl. Acad. Sci. USA* **97**, 103–108 (2000).

3. B. M. Sutherland, P. V. Bennett, N. S. Cintron, P. Guida, M. Hada, H. Schenk, J. Trunk, D. C. Monteleone, J. C. Sutherland, J. Laval, M. Stanislaus and A. Gewirtz, Clustered DNA damages induced in human hematopoietic cells by low doses of ionizing radiation. *J. Radiat. Res.* **43** (Suppl.), S149–S152 (2003).

4. J. O. Blaisdell and S. Wallace, Abortive base-excision repair of radiation-induced clustered DNA lesions in *Escherichia coli*. *Proc. Natl. Acad. Sci. USA* **98**, 7426–7430 (2001).

5. B. M. Sutherland, P. V. Bennett, J. C. Sutherland and J. Laval, Clustered DNA damages induced by X rays in human cells. *Radiat. Res.* **157**, 611–616 (2002).

6. L. F. Povirk, DNA damage and mutagenesis by radiomimetic DNA-cleaving agents: bleomycin, neocarzinostatin and other enediynes. *Mutat. Res.* **355**, 71–89 (1996).

7. P. V. Bennett, N. S. Cintron, L. Gros, J. Laval and B. M. Sutherland, Are endogenous clustered DNA damages induced in human cells? *Free Radic. Biol. Med.* **37**, 488–499 (2004).

8. P. Regulus, B. Duroux, P. A. Bayle, A. Favier, J. Cadet and J. L. Ravanat, Oxidation of the sugar moiety of DNA by ionizing radiation or bleomycin could induce the formation of a cluster DNA lesion. *Proc. Natl. Acad. Sci. USA* **104**, 14032–14037 (2007).

9. B. Paap, D. M. Wilson, III and B. M. Sutherland, Human abasic endonuclease action on multilesion abasic clusters: implications for radiation-induced biological damage. *Nucleic Acids Res.* **36**, 2717–2727 (2008).

10. A. Asaithamby, N. Uematsu, A. Chatterjee, M. D. Story, S. Burma and D. J. Chen, Repair of HZE-particle-induced DNA double-strand breaks in normal human fibroblasts. *Radiat. Res.* **169**, 437–446 (2008).

11. A. G. Georgakilas, P. V. Bennett, D. M. Wilson, 3rd and B. M. Sutherland, Processing of bistranded abasic DNA clusters in gamma-irradiated human hematopoietic cells. *Nucleic Acids Res.* **32**, 5609–5620 (2004).

12. M. Gulston, C. de Lara, T. Jenner, E. Davis and P. O'Neill, Processing of clustered DNA damage generates additional double-strand breaks in mammalian cells post-irradiation. *Nucleic Acids Res.* **32**, 1602–1609 (2004).

13. D. M. Wilson, 3rd, M. Takeshita, A. P. Grollman and B. Demple, Incision activity of human apurinic endonuclease (Ape) at abasic site analogs in DNA. *J. Biol. Chem.* **270**, 16002–16007 (1995).

14. R. Okayasu, M. Okada, A. Okabe, M. Noguchi, K. Takakura and S. Takahashi, Repair of DNA damage induced by accelerated heavy ions in mammalian cells proficient and deficient in the non-homologous end-joining pathway. *Radiat. Res.* **165**, 59–67 (2006).

15. S. Malyarchuk, R. Castore and L. Harrison, DNA repair of clustered lesions in mammalian cells: involvement of non-homologous end-joining. *Nucleic Acids Res.* **36**, 4872–4882 (2008).

16. G. Eot-Houllier, M. Gonera, D. Gasparutto, C. Giustranti and E. Sage, Interplay between DNA N-glycosylases/AP lyases at

17. B. M. Sutherland, P. V. Bennett, E. Weinert, O. Sidorkina and J. Laval, Frequencies and relative levels of clustered damages in DNA exposed to gamma rays in radioquenching vs. nonradioquenching conditions. *Environ. Mol. Mutagen.* **38**, 159–165 (2001).

18. M. Hada and B. M. Sutherland, Spectrum of complex DNA damages depends on the incident radiation. *Radiat. Res.* **165**, 223–230 (2006).

19. E. L. Alpen, P. Powers-Risius, S. B. Curtis, R. DeGuzman and R. J. M. Fry, Fluence-based relative biological effectiveness for charged particle carcinogenesis in mouse harderian gland. *Adv. Space Res.* **14**, 573–581 (1994).

20. W. K. Weyrather, S. Ritter, M. Scholz and G. Kraft, RBE for carbon track-segment irradiation in cell lines of differing repair capacity. *Int. J. Radiat. Biol.* **75**, 1357–1364 (1999).

21. Z. B. Han, H. Suzuki, F. Suzuki, M. Suzuki, Y. Furusawa, T. Kato and M. Ikenaga, Relative biological effectiveness of accelerated heavy ions for induction of morphological transformation in Syrian hamster embryo cells. *J. Radiat. Res. (Tokyo)* **39**, 193–201 (1998).

22. H. Nikjoo, P. O'Neill, W. E. Wilson and D. T. Goodhead, Computational approach for determining the spectrum of DNA damage induced by ionizing radiation. *Radiat. Res.* **156**, 577–583 (2001).

23. H. Terato, R. Tanaka, Y. Nakaarai, T. Nohara, Y. Doi, S. Iwai, R. Hirayama, Y. Furusawa and H. Ide, Quantitative analysis of isolated and clustered DNA damage induced by gamma-rays, carbon ion beams, and iron ion beams. *J. Radiat. Res.* **49**, 133–146 (2008).

24. F. A. Cucinotta, H. Wu, M. R. Shavers and K. George, Radiation dosimetry and biophysical models of space radiation effects. *Gravit. Space Biol. Bull.* **16**, 11–18 (2003).

25. D. J. Keszenman, E. Carmen Candreva and E. Nunes, Cellular and molecular effects of bleomycin are modulated by heat shock in Saccharomyces cerevisiae. *Mutat. Res.* **459**, 29–41 (2000).

26. B. Stenerlow, K. H. Karlsson, B. Cooper and B. Rydberg, Measurement of prompt DNA double-strand breaks in mammalian cells without including heat-labile sites: results for cells deficient in nonhomologous end joining. *Radiat. Res.* **159**, 502–510 (2003).

27. B. Rydberg, Radiation-induced heat-labile sites that convert into DNA double-strand breaks. *Radiat. Res.* **153**, 805–812 (2000).

28. W. Ma, M. Resnick and D. Gordenin, Apn1 and Apn2 endonucleases prevent accumulation of repair-associated DNA breaks in budding yeast as revealed by direct chromosomal analysis. *Nucleic Acids Res.* **36**, 1836–1846 (2008).

29. L. Chen, Kosslak and A. G. Atherly, Mechnical shear of high molecular weight DNA in agarose plugs. *BioTechniques* **16**, 228–229 (1994).

30. J. M. Song, J. R. Milligan and B. M. Sutherland, Bistranded oxidized purine damage clusters: induced in DNA by long-wavelength ultraviolet (290–400 nm) radiation? *Biochemistry* **41**, 8683–8688 (2002).

31. S. Boiteux, E. Gajewski, J. Laval and M. Dizdaroglu, Substrate specificity of the *Escherichia coli* Fpg protein (formamidopyrimidine-DNA glycosylase): excision of purine lesions in DNA produced by ionizing radiation or photosensitization. *Biochemistry* **31**, 106–110 (1992).

32. J. Tchou, H. Kasai, S. Shibutani, M-H. Chung, J. Laval, A. P. Grollman and S. Nishimura, 8-Oxoguanine (8-hydroxyguanine) DNA glycosylase and its substrate specificity. *Proc. Natl. Acad. Sci. USA* **88**, 4690–4694 (1991).

33. A. Hatahet, W. Y. Kow, A. A. Purmal, R. P. Cunningham and S. S. Wallace, New substrates for old enzymes. 5-hydroxy-2′-deoxycytidine and 5-hydroxy-2′-deoxyuridine are substrates for *Escherichia coli* endonuclease III and formamidopyrimidine DNA N-glycosylase, while 5-hydroxy-2′-deoxyuridine is a

substrate for uracil DNA N-glycosylase. *J. Biol. Chem.* **269**, 18814–18820 (1994).

34. J. Jurado, M. Saparbaev, T. J. Matray, M. M. Greenberg and J. Laval, The ring fragmentation product of thymidine C5-hydrate when present in DNA is repaired by the *Escherichia coli* Fpg and Nth proteins. *Biochemistry* **37**, 7757–7763 (1998).

35. S. S. Wallace, Enzymatic processing of radiation-induced free radical damage in DNA. *Radiat. Res.* **150** (Suppl.), S60–S79 (1998).

36. M. Haring, H. Rudiger, B. Demple, S. Boiteux and B. Epe, Recognition of oxidized abasic sites by repair endonucleases. *Nucleic Acids Res.* **22**, 2010–2015 (1994).

37. H. Ide, K. Tedzuka, H. Shimzu, Y. Kumura, A. A. Purmal, S. S. Wallace and Y. W. Kow, a-Deoxyadenosine, a major anoxic radiolysis product of adenine in DNA, is a substrate for *Escherichia coli* endonuclease IV. *Biochemistry* **33**, 7842–7847 (1994).

38. A. Ishchenko, G. Sanz, C. Privezentzev, A. Maksimenko and M. Saparbaev, Characterisation of new substrate specificities of *Escherichia coli* and *Saccharomyces cerevisiae* AP endonucleases. *Nucleic Acids Res.* **31**, 6344–6353 (2003).

39. J. C. Sutherland, B. Lin, D. C. Monteleone, J. Mugavero, B. M. Sutherland and J. Trunk, Electronic imaging system for direct and rapid quantitation of fluorescence from electrophoretic gels: application to ethidium bromide-stained DNA. *Anal. Biochem.* **163**, 446–457 (1987).

40. B. M. Sutherland, P. V. Bennett, A. G. Georgakilas and J. C. Sutherland, Evaluation of number average length analysis in quantifying double strand breaks in genomic DNAs. *Biochemistry* **42**, 3375–3384 (2003).

41. K. M. Prise, C. H. Pullar and B. D. Michael, A study of endonuclease III-sensitive sites in irradiated DNA: detection of alpha-particle-induced oxidative damage. *Carcinogenesis* **20**, 905–909 (1999).

42. S. G. Kozmin, Y. Sedletska, A. Reynaud-Angelin, D. Gasparutto and E. Sage, The formation of double-strand breaks at multiply damaged sites is driven by the kinetics of excision/incision at base damage in eukaryotic cells. *Nucleic Acids Res.* **37**, 1767–1777 (2010).

43. D. T. Goodhead, Molecular and cell models of biological effects of heavy ion radiation. *Radiat. Environ. Biophys.* **34**, 67–72 (1995).

44. J. Milligan, J. Aguilera, T. Nguyen, R. Paglinawan and J. Ward, DNA strand-break yields after post-irradiation incubation with base excision repair endonucleases implicate hydroxyl radical pairs in double-strand break formation. *Int. J. Radiat. Biol.* **76**, 1475–1483 (2000).

45. B. Gervais, M. Beuve, G. H. Olivera and M. E. Galassi, Numerical simulation of multiple ionization and high LET effects in liquid water radiolysis. *Radiat. Phys. Chem.* **75**, 493–513 (2006).

46. J. A. LaVerne, Track effects of heavy ions in liquid water. *Radiat. Res.* **153**, 487–496 (2000).

47. J. A. La Verne, Radical and molecular yields in the radiolysis of water with carbon ions. *Int. J. Radiat. Appl. Instrum. C Radiat. Phys. Chem.* **34**, 135–143 (1989).

48. J. Kiefer, R. Egenolf and S. Ikpeme, Heavy ion-induced DNA double-strand breaks in yeast. *Radiat. Res.* **157**, 141–148 (2002).

49. A. Urushibara, N. Shikazono, P. O'Neill, K. Fujii, S. Wada and A. Yokoya, LET dependence of the yield of single-, double-strand breaks and base lesions in fully hydrated plasmid DNA films by $^4He^{2+}$ ion irradiation. *Int. J. Radiat. Biol.* **84**, 23–33 (2008).

50. N. Shikazono, M. Noguchi, K. Fujii, A. Urushibara and A. Yokoya, The yield, processing, and biological consequences of clustered DNA damage induced by ionizing radiation. *J. Radiat. Res.* **50**, 27–36 (2009).